



Doubly Selective Fading Channel Modeling and Data Comparison for OFDM System

{Abdelrahman Marconi^{*}, Hisham Dahshan[†]}[‡]

Abstract: The mathematical model and the equivalent matrix representation of the doubly selective fading channel is proposed, A MATLAB based simulation is used to perform data comparison with the results of the MATLAB channel toolbox, based on both:

- *Deterministic functions* (System functions).
- *Stochastic functions* (Autocorrelation functions).

Keywords: Rayleigh fading, Doubly selective channel, wireless Channel, Doppler, MATLAB, OFDM, Channel Matrix.

1. Introduction

Wireless channel may suffer from a variation in the signal strength in both time and frequency, those variations can be divided into:

- Large scale fading, which arises from the motion along large distance, e.g. distance in the order of the cell size.
- Small scale fading, which arises from the motion along small distance in the order of the carrier wavelength.

Large scale fading is more relevant to issues such as cell-site planning. Small scale multipath fading is more relevant to the design of reliable and efficient communication systems, therefore, our interest will be for the small scale fading [8].

A defining characterizing of the small scale fading is:

- Time selectivity (Frequency dispersion), which arises from the varying nature of the channel in the time due to the Doppler frequency.
- Frequency selectivity (Time dispersion), which arises from the multipath propagation.

Orthogonal Frequency-Division Multiplexing (OFDM) is a robust modulation technique against the frequency selectivity, therefore, it pervades most of the telecommunication standards developed in the last two decades, such as DAB, DVB-T/H, Wi-Fi (IEEE 802.11a/n), and UMTS-LTE, etc. [3], [4], [5] and [6].

The simulation of an OFDM system needs to model the channel, either in time or frequency. MATLAB provides a toolbox for simulating the wireless channel. This tool allows using the channel in time domain only. Therefore, it stores the channel pathgains only and hide other channel data such as the frequency response data. Moreover, it doesn't provide the tapgains, which are necessary in the OFDM systems.

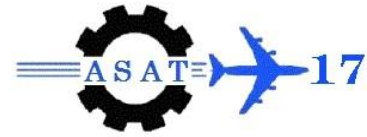
Most of the wireless channel models such as Typical Urban channel model (Tux), Rural Area channel model (Rax) and Hilly Terrain channel model (HTx) [1] provide the relative delays and

* marconi@mtc.edu.eg

† hdahshan@mtc.edu.eg

‡ Egyptian Armed Forces, Egypt.

17th International Conference on
AEROSPACE SCIENCES & AVIATION TECHNOLOGY,
ASAT - 17 – April 11 - 13, 2017, E-Mail: asat@mtc.edu.eg
Military Technical College, Kobry Elkobbah, Cairo, Egypt
Tel: +(202) 24025292 – 24036138, Fax: +(202) 22621908



average relative power for each path, which isn't convenient to be used directly in the simulations, instead we need to get the average relative power for each tap (tapgains).

Therefore, we build our own tool, which allows us to explore more data about the channel in both time and frequency domains, and to be capable of calculating the tapgains from the pathgains.

In order to calculate the tapgains, we need to model the channel in both mathematical and matrices forms.

Also, a MATLAB based approach is presented for the doubly selective fading channel and is compared with the MATLAB channel toolbox.

2. Physical Modeling of Multipath Fading Channel

Clarke's model is commonly used to statistically model the flat fading channel, in which it is assumed that the transmitter is fixed with vertically polarized antenna, and the transmitted signal is scattered by stationary objects around the mobile antenna, the field incident on the mobile antenna results from waves equal in the average amplitude and differ in phase [2], This models the situation when the scatterers are located uniformly in a ring around the mobile.

2.1. Spectral Shape Due to The Doppler Spread in Clarke's Model

If the scattered signal is a continuous wave signal of frequency with a maximum doppler shift, then the power spectral density can be expressed as [8]:

$$S(f) = \begin{cases} k_1 [1 - (f / f_d)^2]^{-1/2} & |f| \leq f_d = V / \lambda \\ 0 & \text{Otherwise} \end{cases} \quad (1)$$

where k_1 is a constant, V is the receiver velocity and λ is the signal wavelength. The corresponding autocorrelation R_0 function can be expressed as:

$$R_0[\tau] = k_2 J_0(\tau \pi f_d / W) \quad (2)$$

where τ is the time delay, k_2 is a constant, J_0 is the zeroth-order Bessel function of the first kind and W is the signal bandwidth.

3. Wireless Channel Model

The wireless channel can be modeled as (Deterministic or Random) Linear Time-Variant (LTV) filter characterized by one of the following four deterministic system function [10] and [12]:

1. Time-variant impulse response $h(t, \tau)$.
2. Doppler-variant transfer function $B(v, f)$.
3. Time-variant transfer function $H(t, f)$.
4. Doppler-variant impulse response $S(v, \tau)$.

The relations between those four deterministic system function is shown in Figure 1.

Therefore, wireless channel can be stochastically described by the autocorrelation functions (ACF).

1. Scattering Function.
2. Delay Cross Spectral Density.
3. Time Frequency Correlation Function.
4. Doppler Cross Spectral Density.

Figure 2 shows the relations between the ACF.

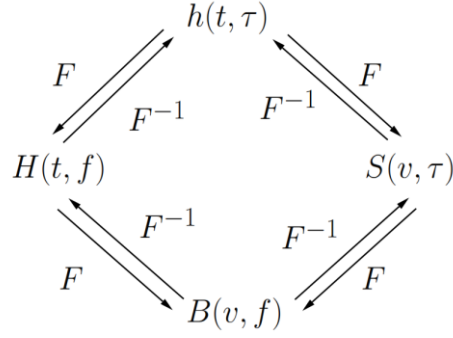


Fig. 1 Relations between deterministic system function.

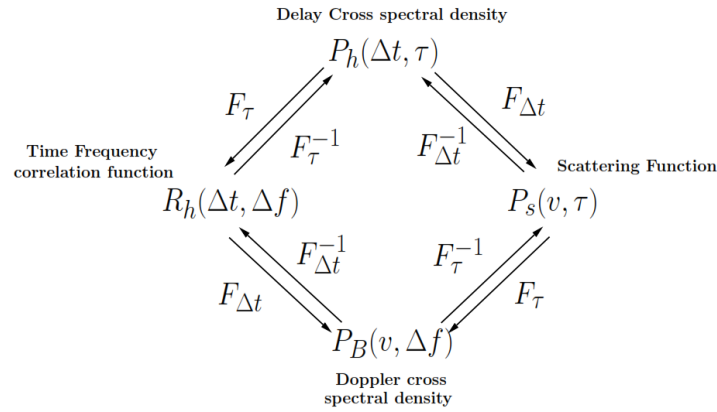


Fig. 2 The magnitude of the Doppler-variant impulse response for time variant multipath channel.

4. Deterministic Channel Representation

The wireless channel can be described by one of the following four system functions.

4.1. Time-Variant Impulse Response $h(t, \tau)$

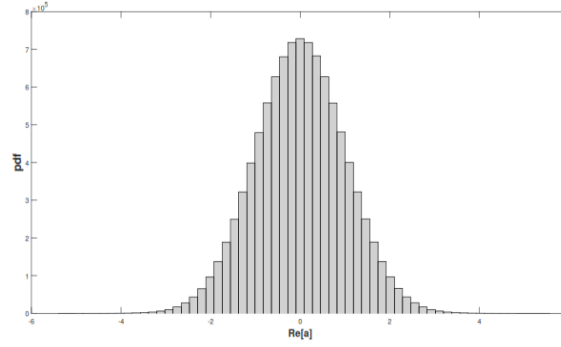
The impulse response of the doubly selective channel with M taps is represented as a function in both time and delay [11]:

$$c(t, \tau) = \sum_m a_m(t) \delta(\tau - \tau_m(t)) \quad (3)$$

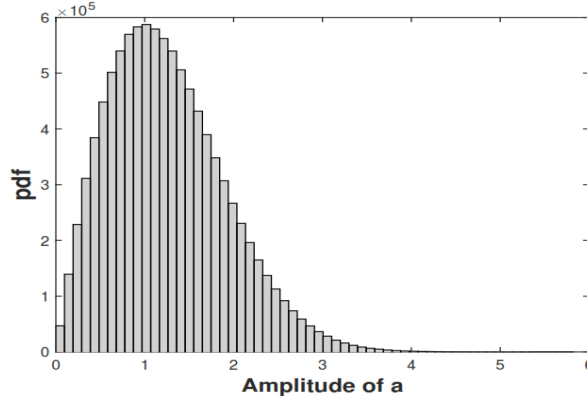
where $\tau_m(t)$ is the delay of the m tap, Figure 4 shows the effect of each path on the different channel taps. Channel taps are uniformly distributed along the time with separation time equals to the sampling time T_s , channel paths aren't in necessary to be at the same time instant as the channel taps, they aren't uniformly distributed along the time, Therefore, may locate in between 2 successive taps, the average tapgains are calculated from the resultant contribution of all paths at each tap.

a_m is a complex random variable, which has both real and imaginary values with a zero mean Gaussian distribution. This is a consequence of the central limit theorem: When superimposing

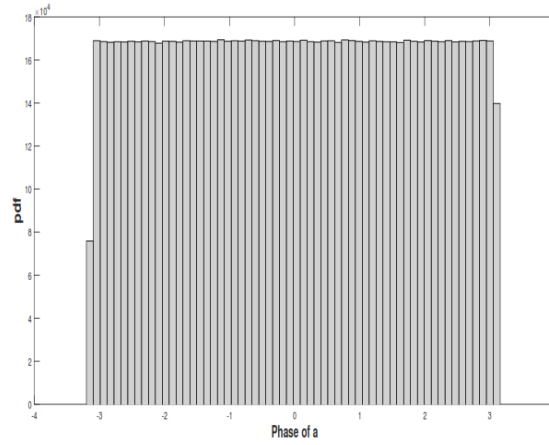
N statistically independent random variables, none of which is dominant, the associated probability density function (pdf) approaches a normal distribution for $N \rightarrow \infty$ Figure 3a [12].



a. [The Histogram of the real values of a_m is a Gaussian pdf.]



b. [The amplitude of a_m is a Rayleigh pdf.]



c. [The phase of a_m is a uniform pdf]

Fig. 3 The pdf Histogram of the channel pathgain's real part, imaginary part, amplitude and phase

Therefore, a_m has an amplitude with Rayleigh distribution, hence we refer to this case simply as "Rayleigh fading" Figure 3b, and the phase of a_m is uniformly distributed Figure 3c. We can express the LPF h_{lpf} and the channel as two cascaded systems which is equivalent to the system impulse response $h(t, \tau)$, see [11] and [13]:

$$h_{lpf} = \text{sinc}(wt) \quad (4)$$

where $W/2$ is the baseband signal bandwidth.

$$h(t, \tau) = h_{lpf} * c(t, \tau) \quad (5)$$

$$h(t, \tau) = \int_{-\infty}^{\infty} c(t, \tau) \text{sinc}(\omega t - \omega \tau) d\tau \quad (6)$$

$$h(t, \tau) = \sum_m a_m(t) \int_{-\infty}^{\infty} \delta(\tau - \tau_m(t)) \text{sinc}(\omega t - \omega \tau) d\tau \quad (7)$$

By applying sifting property

$$h(t, \tau) = \sum_m a_m(t) \text{sinc}(\omega t - \omega \tau_m(t)) \quad (8)$$

Figure 4 shows the magnitude of the channel impulse response (IR) $|h(t, \tau)|$ in different cases of time and frequency selectivity compared with the channel time variant transfers function (TF) $|H(t, \tau)|$.

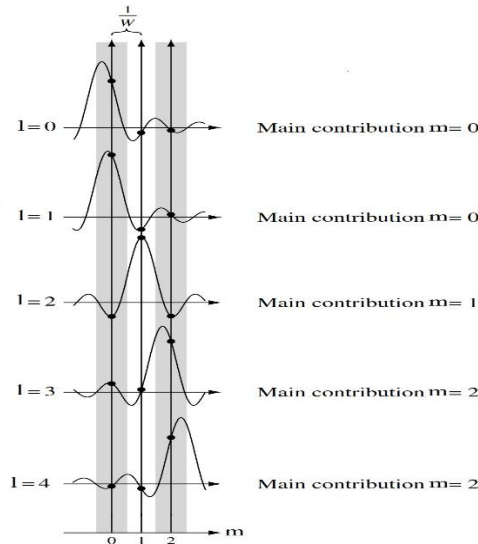


Fig. 4 The effect of each channel path on the channel taps.

4.2. Time-Variant Transfer Function $H(t, f)$

The Time-variant TF is the result of applying 1D Fourier transform to the channel IR $h(t, \tau)$ with respect to the variable τ eqn. 9, shown in Figure 8.

$$H(t, f) = \frac{1}{\sqrt{N}} \int_0^{\tau_{max}} h(t, \tau) e^{(-j\frac{2\pi f}{N}\tau)} d\tau \quad (9)$$

4.3. Doppler-Variant Transfer Function $B(v, f)$

The Doppler Variant TF is the result of applying 1D Fourier transform to the channel time-variant TF $H(t, f)$ with respect to the variable t eqn10.

$$B(v, f) = \frac{1}{\sqrt{N}} \int_0^t H(t, f) e^{(-j\frac{2\pi t}{N}v)} dt \quad (10)$$

Figure 9 shows the magnitude of the channel Doppler Variant TF $B(v, f)$ in different cases of time and frequency selectivity.

4.4. Doppler-Variant Impulse Response $S(v, \tau)$

The Doppler-variant IR $S(v, \tau)$ is the result of applying 1D Fourier transform to the channel Doppler Variant TF $B(v, f)$ with respect to the variable f eqn11.

$$S(v, \tau) = \frac{1}{\sqrt{N}} \int_0^{\tau_{max}} B(v, f) e^{(-j\frac{2\pi f}{N}\tau)} d\tau \quad (11)$$

Figure 4 shows the magnitude of Doppler-variant IR $S(v, \tau)$ in the cases of both time and frequency selectivity.

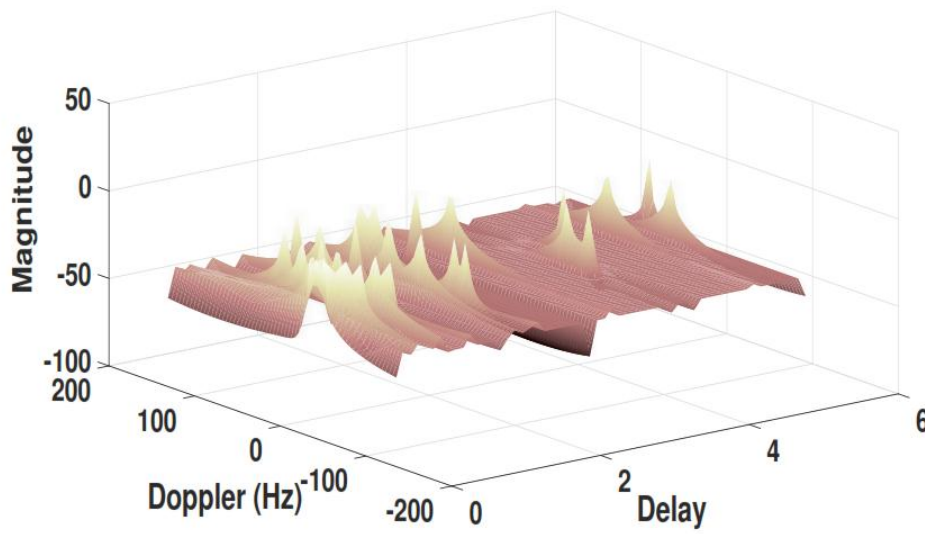


Fig. 5 The magnitude of the Doppler-variant impulse response $|S(v, \tau)|$ for time variant multipath channel.

5. Channel Matrix Representation for OFDM System

Assume an OFDM system with K subcarriers, each subcarrier contains a modulated symbols X , drawn from M-QAM alphabet [9].

5.1. OFDM Time Domain Model

The sampled time domain signal can be expressed as the IDFT of those symbols as:

$$x[n] = \frac{1}{\sqrt{N}} \sum_{k=0}^{N-1} X[k] e^{j\frac{2\pi n k}{N}} \quad (12)$$

where N is the IDFT length. then the received signal in time domain $y[n]$ can be expressed as [11]:

$$y[n] = h(n, m) * x[n] \quad (13)$$

$$y[n] = \sum_{m=0}^M h[n, m] x[n - m] \quad (14)$$

Eqn. 14 represents a discrete circular convolution [14], and can be represented in matrix form as follows:

$$\mathbf{y} = \mathbf{h}\mathbf{x} \quad (15)$$

where \mathbf{y} is the received time domain data vector of size $N \times 1$, \mathbf{h} is the channel impulse response matrix of size $N \times N$ and \mathbf{x} is the M-QAM symbols contained in the OFDM symbol after IDFT with size $N \times 1$.

5.2. OFDM Frequency Domain Model

The mathematical representation of the sampled received signal $Y[v]$ can be expressed as:

$$Y[v] = \frac{1}{\sqrt{N}} \sum_{n=0}^{N-1} y[n] e^{-j \frac{2\pi n}{N} v} \quad (16)$$

where v represents the discrete Doppler frequency.

$$Y[v] = \frac{1}{\sqrt{N}} \sum_{n=0}^{N-1} \left(\sum_{m=0}^M h[n, m] x[n - m] \right) e^{-j \frac{2\pi n}{N} v} \quad (17)$$

$$Y[v] = \frac{1}{\sqrt{N}} \sum_{n=0}^{N-1} \left(\sum_{m=0}^M h[n, m] \frac{1}{\sqrt{N}} \sum_{k=0}^{N-1} X[k] e^{j \frac{2\pi(n-m)k}{N}} \right) e^{-j \frac{2\pi v}{N} n} \quad (18)$$

$$Y[v] = \sum_{n=0}^{N-1} \left(\frac{1}{\sqrt{N}} \sum_{m=0}^M \left(\frac{1}{\sqrt{N}} \sum_{k=0}^{N-1} h[n, m] e^{j \frac{-2\pi(v-k)n}{N}} \right) e^{-j \frac{2\pi k}{N} m} \right) X[k] \quad (19)$$

$$Y[v] = \sum_{n=0}^{N-1} \left(\frac{1}{\sqrt{N}} \sum_{m=0}^M \left(\frac{1}{\sqrt{N}} \sum_{k=0}^{N-1} h[n, m] e^{-j \frac{2\pi k}{N} m} \right) e^{j \frac{-2\pi(v-k)n}{N}} \right) X[k] \quad (20)$$

$$Y[v] = \sum_{n=0}^{N-1} \left(\frac{1}{\sqrt{N}} \sum_{m=0}^M H[n, k] e^{-j \frac{2\pi(v-k)n}{N}} \right) X[k] \quad (21)$$

$$Y[v] = \sum_{n=0}^{N-1} B[v - k, k] X[k] \quad (22)$$

then

$$\mathbf{Y} = \mathbf{B}\mathbf{X} \quad (23)$$

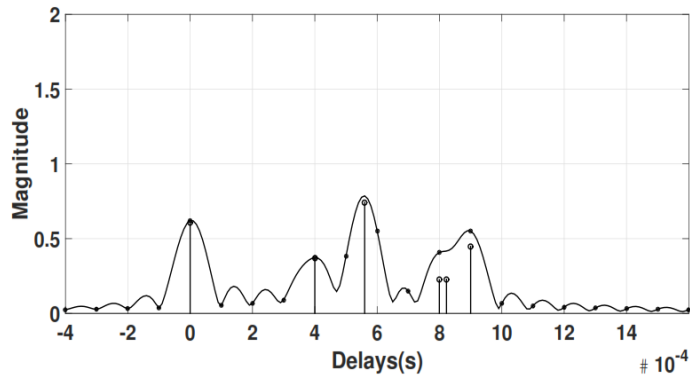
where \mathbf{Y} is the received frequency domain data vector of size $N \times 1$, \mathbf{B} is the channel doppler variant TF matrix of size $N \times N$ and \mathbf{X} is the M-QAM symbols contained in the OFDM symbol with size $N \times 1$.

6. Data Comparison with MATLAB Channel Toolbox

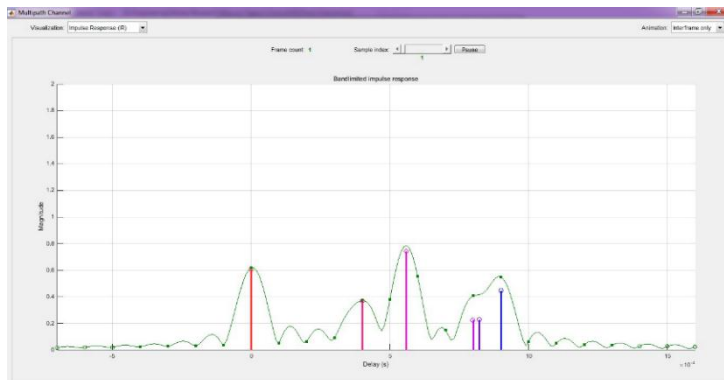
MATLAB provides a channel toolbox in which data is stored only in the time domain, we compare our results with the results obtained from the MATLAB toolbox.

Figure 6 shows a multipath channel impulse response for the first instant of the channel, a comparison between result obtained from MATLAB channel toolbox Figure 5, and our own simulation result Figure 5.

Figure 7 shows a frequency selective channel transfer function for the first sample of the channel, a comparison between result obtained from MATLAB channel toolbox Figure 8, and our own simulation result Figure 6.

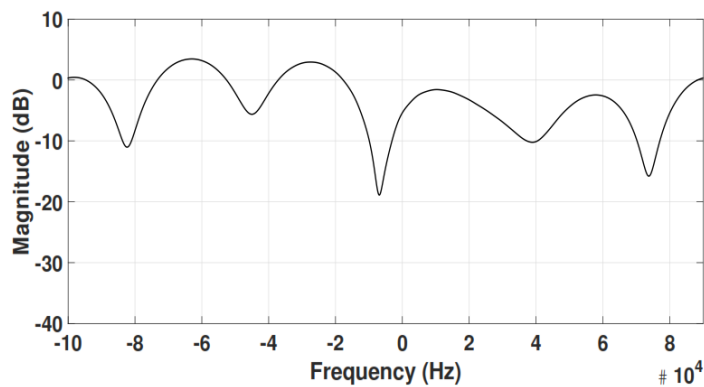


a. [Simulated channel.]

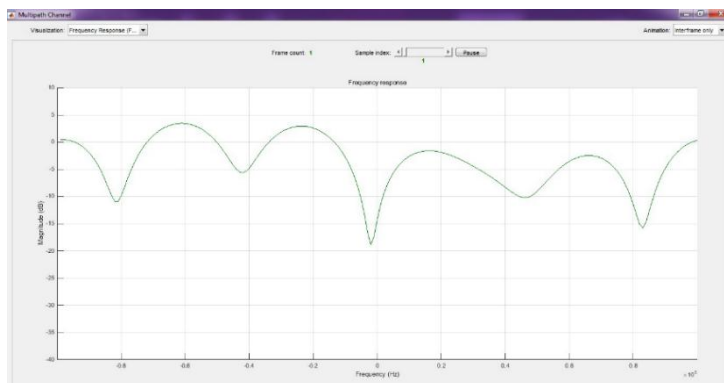


b. [Data from MATLAB tool *channel vis.*]

Fig. 6 Data verification with MATLAB object rayleighchan of time invariant multipath channel impulse response

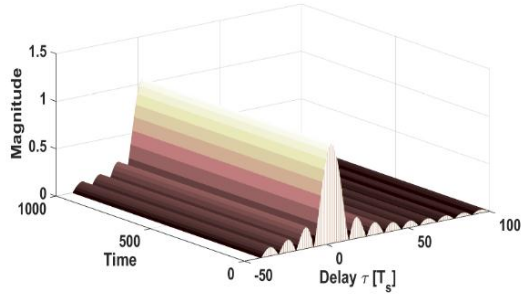


a. [Simulated channel.]

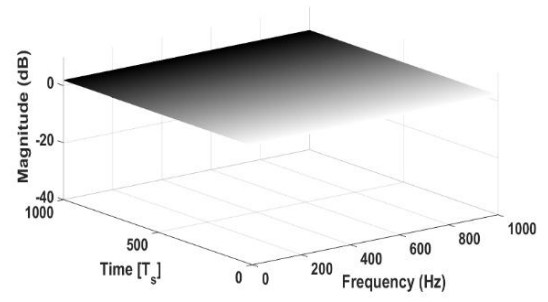


b. [Data from MATLAB tool *channel vis.*]

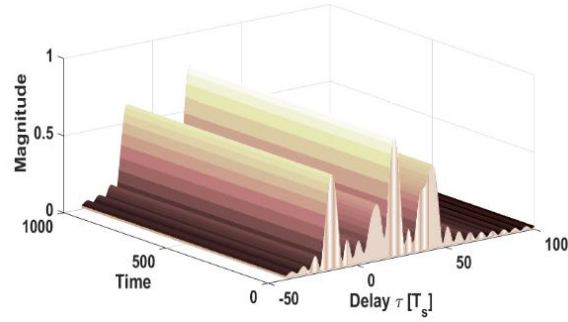
Fig. 7 Data verification with MATLAB object rayleighchan of time invariant multipath channel frequency response



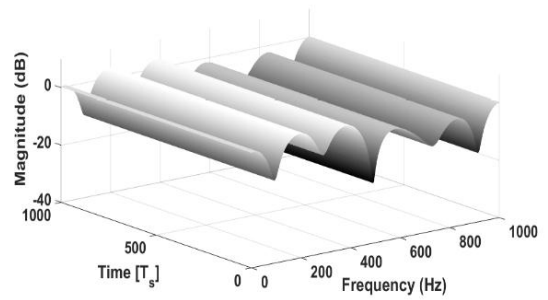
(a) The magnitude of the IR $|h(t, \tau)|$ for time invariant single path channel.



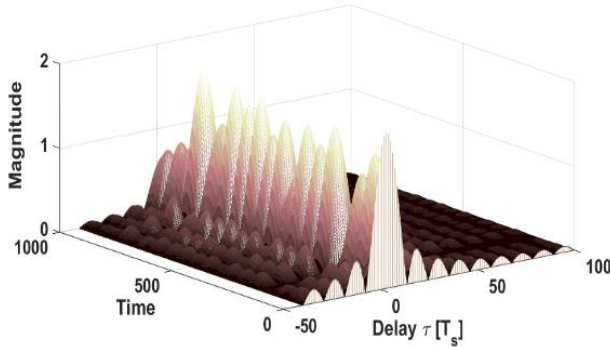
(b) The magnitude of the TF $|H(t, f)|$ for time Invariant single path channel.



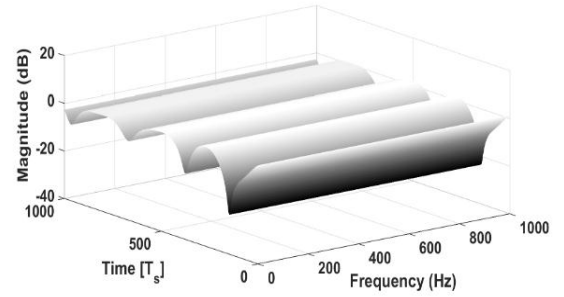
(c) The magnitude of the IR $|h(t, \tau)|$ for time invariant multipath channel.



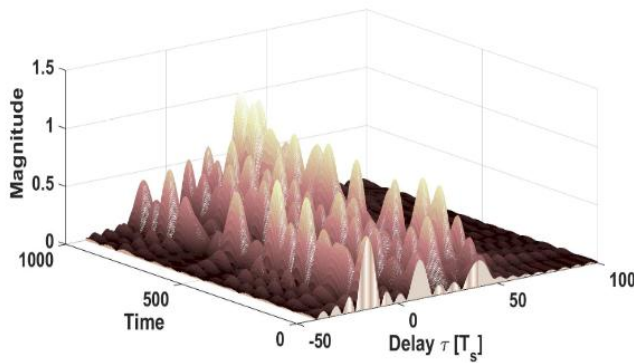
(d) The magnitude of TF $|H(t, f)|$ for time invariant multipath channel.



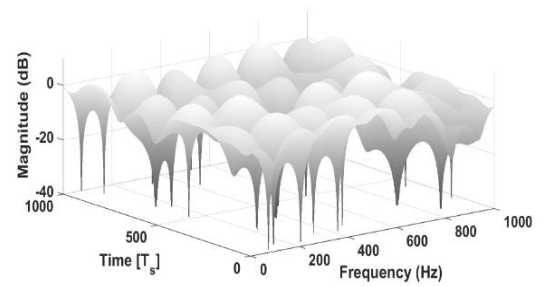
(e) The magnitude of the IR $|h(t, \tau)|$ for time variant single path channel.



(f) The magnitude of TF $|H(t, f)|$ for time variant single path channel.



(g) The magnitude of the IR $|h(t, \tau)|$ for time variant multipath channel.



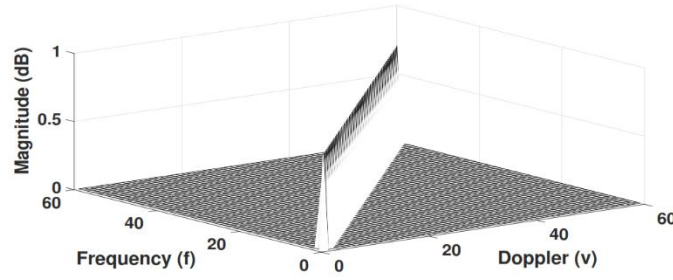
(h) The magnitude of TF $|H(t, f)|$ for time variant multipath channel.

Fig. 8. The magnitude of the channel IR $|h(t, \tau)|$ and $|H(t, f)|$ in different cases of time and frequency selectivity.

$$\begin{bmatrix} h[0,0] & 0 & \dots & 0 \\ 0 & h[0,0] & \ddots & \vdots \\ \vdots & \vdots & \ddots & \vdots \\ 0 & \dots & \dots & h[0,0] \end{bmatrix} \quad \begin{bmatrix} B(0,0) & 0 & \dots & 0 \\ 0 & B(0,0) & \dots & 0 \\ \vdots & \vdots & \ddots & \vdots \\ 0 & 0 & \dots & B(0,0) \end{bmatrix}$$

(a) [Time domain matrix representation of the time invariant single path channel.]

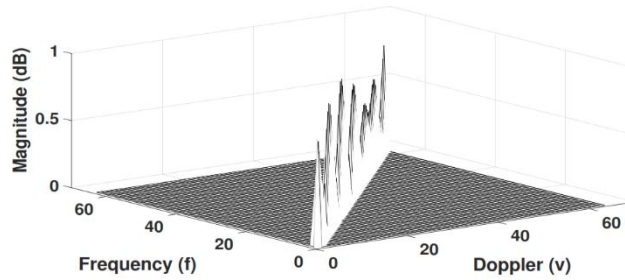
(b) [frequency domain matrix representation of the time invariant single path channel.]


 (c) [The magnitude of the Doppler-variant TF $B(v; f)$ for time invariant single path channel.]

$$\begin{bmatrix} h[0,0] & 0 & \dots & \dots & 0 \\ h[0,1] & h[0,0] & \ddots & \ddots & \vdots \\ \vdots & \vdots & \ddots & \ddots & \vdots \\ h[0,N-1] & h[0,N-2] & h[0,N-2] & \dots & h[0,0] \end{bmatrix} \quad \begin{bmatrix} B(0,0) & 0 & \dots & 0 \\ 0 & B(0,1) & \dots & 0 \\ \vdots & \vdots & \ddots & \vdots \\ 0 & 0 & \dots & B(0,N-1) \end{bmatrix}$$

(d) [Time domain matrix representation of the time invariant multipath channel.]

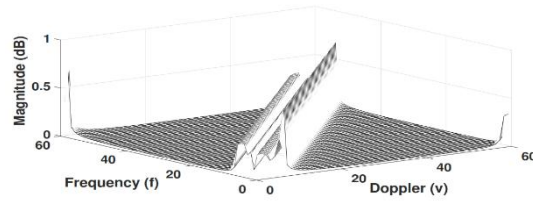
(e) [Frequency domain matrix representation of the time invariant multipath channel.]


 (f) [The magnitude of the Doppler-variant TF $B(v, f)$ for time invariant multipath channel.]

$$\begin{bmatrix} h[0,0] & 0 & \cdots & 0 \\ 0 & h[1,0] & \ddots & \vdots \\ \vdots & \vdots & \ddots & \vdots \\ 0 & \cdots & \cdots & h[N-1,0] \end{bmatrix} \quad \begin{bmatrix} B(0,0) & B(-1,0) & \cdots & B(1-N,0) \\ B(1,0) & B(0,0) & \cdots & B(2-N,0) \\ \vdots & \vdots & \ddots & \vdots \\ B(N-1,0) & B(N-2,0) & \cdots & B(0,0) \end{bmatrix}$$

(g) [Time domain matrix representation of the time variant single path channel.]

(h) [Frequency domain matrix representation the time variant single path channel]

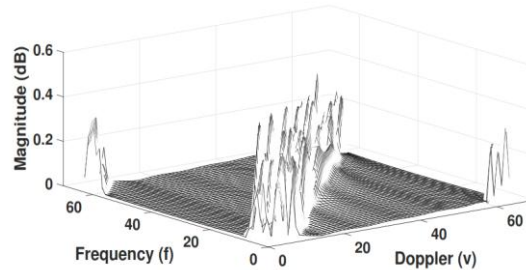


(i) [The magnitude of the Doppler-variant TF for $B(v, f)$ time variant single path channel.]

$$\begin{bmatrix} h[0,0] & 0 & \cdots & 0 \\ h[1,1] & h[1,0] & \ddots & \vdots \\ \vdots & \vdots & \ddots & \vdots \\ h[N-1,N-1] & h[N-1,N-2] & \cdots & h[N-1,0] \end{bmatrix} \quad \begin{bmatrix} B(0,0) & B(-1,1) & \cdots & B(1-N,N-1) \\ B(1,0) & B(0,1) & \cdots & B(2-N,N-1) \\ \vdots & \vdots & \ddots & \vdots \\ B(N-1,0) & B(N-2,1) & \cdots & B(0,N-1) \end{bmatrix}$$

(j) [Time domain matrix representation of the time variant multipath channel.]

(k) [Frequency domain matrix representation of the time variant multipath channel.]



(l) [The magnitude of the Doppler-variant TF $B(v, f)$ for time variant multipath channel.]

Fig. 9 The magnitude of the channel Doppler-variant TF $B(v, f)$ in different cases of time and frequency selectivity and the corresponding matrix representation in time and frequency domains

7. Conclusion

A mathematical and a matrix representation of the doubly selective channel is proposed, in both time and frequency domains.

MATLAB based simulations is performed using our own channel toolbox compared with the MATLAB built in channel toolbox.

8. References

- [1] 3rd Generation Partnership Project; Technical Specification Group GSM/EDGE Radio Access Network; Radio transmission and reception (Release 1999), 3GPP TS 05.05 V8.20.0, Annex C.3 Propagation models.
- [2] R. H. Clarke, "A statistical theory of mobile-radio reception" Bell Sys. Tech. J., vol. 47, no. 6, July-Aug. 1968.
- [3] ETSI European Telecommunications Standards Institute, Digital audio broadcasting (DAB): data broadcasting MPEG 2 TS streaming, ETSI TS 102 427, V1.1.1, Thereforephia Antipolis, France, July 2005.
- [4] ETSI European Telecommunications Standards Institute, Digital video broadcasting (DVB): framing structure channel coding and modulation for digital terrestrial television, ETSI EN 300 744, V1.5.1, Thereforephia Antipolis, France, November 2004.
- [5] ETSI, European Telecommunications Standards Institute, Digital Video Broadcasting (DVB), Frame structure channel coding and modulation for a second generation digital terrestrial television broadcasting system (DVB-T2), ETSI EN 302 755, V1.1.1, Thereforephia Antipolis, France, September 2009.
- [6] IEEE, Institute of Electrical and Electronics Engineers, Part 11: wireless LAN medium access control (MAC) and physical layer (PHY): high-speed physical layer in the 5 GHz band, IEEE Std 802.11a-1999, New York, NY, December 1999.
- [7] 3GPP 3rd Generation Partnership Project, Technical group Radio Access Network, Evolved Universal Terrestrial Radio Access (EUTRA): Physical channels and modulation, 3GPP TS 36.211 V8.5.0, Thereforephia Antipolis, France, December 2008.
- [8] T. S. Rappaport, "Wireless Communication", 2002.
- [9] R. Prasad, "OFDM for Wireless Communications Systems", 2004.
- [10] P. A. Bello, "Characterization of randomly time-variant linear channels" IEEE Trans. Commun. Syst., vol. CS-11, no. 4, Dec. 1963.
- [11] D. Tse, P. Viswanath, "Fundamentals of Wireless Communication", 2005.
- [12] Andreas F. Molisch, Wireless Communications, 2011.
- [13] M. C. Jeruchim, P. Balaban, and K. S. Shanmugan, Simulation of Communication Systems Modeling, Methodology, and Techniques, Kluwer Academic/Plenum Publishers, 2nd edition, 2000.
- [14] A.V. Oppenheim, R.W. Schaffer, Discrete-Time Signal Processing, Prentice-Hall, Englewood Cliffs, 1989.